Eugeniusz KURGAN, Piotr GAS

AGH University of Science and Technology

doi:10.15199/48.2015.01.37

Simulation of the electromagnetic field and temperature distribution in human tissue in RF hyperthermia

***Abstract**. In this publication colloid with superparamagnetic nanoparticles is considered. Also Brown and Néel relaxation processes were taken into account. With assumption that effective value of the field in particle is equal to the exciting field, formulae for power losses in ferrofluid is derived. At the end discussion of the influence of the different particle parameters on the generated power is given.*

Streszczenie**. W artykule tym przedstawiono sposób obliczania mocy wytwarzanej przez koloid zawierający superparamagnetyczne nanocząsteczki. Zjawisko relaksacji Browna i Néele'a zostało uwzględnione przy wyprowadzaniu wzorów na moc. Na koniec przedyskutowano wpływ różnych parametrów cząsteczki na wytworzoną moc.* (Symulacja pola elektromagnetycznego i rozkładu temperatury w tkance ludzkiej w czasie RF hipertermii***)

Keywords: nanoparticle hyperthermia, finite element method, Brown and Néel relaxation processes
Słowa kluczowe: hipertermia nanocząsteczek, metoda elementów skończonych, zjawisko relaksacji Browna i Néele'a

Introduction

The ability of magnetic nanoparticles to performance as effective heating sources for magnetic hyperthermia has been showed many years ago [1]. However, the mechanisms and limits for supplying the generated energy to intracellular spaces are still questions to discuss [2]. The therapeutic application of magnetic hyperthermia consist in externally increasing the temperature of a tissue with a tumour through alternating magnetic fields acting on magnetic nanoparticles previously inserted in that tissue. The safety of magnetic hyperthermia in comparison with microwave or eddy current based hyperthermia is associated with the frequency region (f < 1MHz) of the electromagnetic radiation used by this type of hyperthermia, where the heating effects on living healthy tissues are negligible. The mechanism of the energy dissipation when a magnetic colloid is located in an AC magnetic field has been extensively studied for different particle radiuses, colloid viscosity, volume fraction of particles in suspension and magnetic field strengths.

Most of the experimental and theoretical studies consider single-domain particles, and thus the discussion of heat generation method is concerned to Brownian and Néel relaxation mechanisms. The prevailing picture today is that power absorption takes place mainly through Néel relaxation process of the magnetic moments, since energy losses from mechanical rotation of the particles, acting against viscous forces of the liquid medium (Brownian losses) cannot contribute at those frequency ranges used magnetic hyperthermia [5].

Different heating methods are used to heat the superficial and deep placed tumors. Resistive heating with external electrodes, microwaves or ultrasound are usually used. Such techniques, however, may cause problems in heating deeply situated tumors, due to unavoidable over-heating adjacent healthy tissues. In recent years interest in improving hyperthermia techniques has gained substantial attention in searching for new methods that can result in depth and uniform tissue heating. Invasive methods include heating with deep implanted electrodes, invasive microwave antennas, thermal seed heating, etc [10].

A main advantage of electromagnetic hyperthermia is its ability to control the destruction process by a single electro-magnetic applicator. In ideal case, concentrating power on a tumor selectively, heats it to temperatures high enough to destroy cancerous cells without overheating and damaging the surrounding healthy tissues.

To apply the induction heating ability for magnetic hyperthermia, the magnetic fluids are usually crated as finite-size particles, and subjected to an AC magnetic field with the intensity H_{ex} < 16 kA/m and frequency f < 1 MHz, which are typically used in clinical hyperthermia treatments. However, the influence of field distribution in nanoparticles on the heating performances of magnetic fluids is rarely discussed in related studies [7].

The amount of magnetic particles required to generate the needed temperatures depends to a large degree on the method of administration. Direct injection permits for considerably greater quantities of magnetic material to be placed in a tumour than in methods using intravascular administration or antibody targeting, although the latter two may have other advantages. A realistic supposition is that circa 5 – 10 mg of magnetic material placed in each cm^3 of the tumor tissue is adequate for magnetic hyperthermia in human patients [8].

In this article influence of human tissue parameters on electromagnetic field, generated power losses and temperature distribution is considered. In order to calculate a full investigation of the temperature variation in human tissues, one needs to take into account the tissue composition, the blood perfusion rate, the heat conduction effects of various tissues, and the heat generation due to the metabolic processes. Also influence of nanoparticle parameters on temperature distribution is examined.

Magnetisation of particle

Over the last years the hyperthermia has been based on magnetic colloids, where the magnetic material consists of superparamagnetic nanoparticles suspended in water or a hydrocarbon fluid to create a magnetic fluid known also as ferrofluid. When a superparamagnetic particle is removed from a magnetic field its magnetization vector relaxes back to zero because of the external thermal energy of the fluid suspension. This relaxation is due either to the physical rotation of the particles themselves within the fluid, or rotation of magnetic moments within each particle. Rotation of the whole particles in colloidal suspension is known as Brownian rotation while rotation of the moment within each particle, while particle itself is motionless, is referred as Néel relaxation. Each of these processes is described by a relaxation time: τ_B for the Brownian motion, which depends on the hydrodynamic properties of the fluid; while τ_N for the Néel process, which is influenced by the magnetic anisotropy energy of the superparamagnetic particles relative to the thermal energy. Both Brownian and Néel relaxation movements may appear in a ferrofluid, whereas only τ_N is significant where no physical rotation of the particle takes place. The relaxation times τ_B and τ_N depend in different way from particle size. Losses of energy caused by Brownian rotation have maximum value at a lower frequency than are those due to Néel relaxation for a given particle size [1].

For small exciting magnetic field amplitudes, and assuming lack of interactions between the super-paramagnetic particles, which occur in colloidal suspension, the properties of the ferrofluid to an exciting AC field can be described in terms of its complex susceptibility $\chi = \chi' - \mathrm{j}\chi''$, where both χ' and χ'' are frequency dependent. The out-of-phase χ'' part of susceptibility component is a source of the heat generation given by

$$P = \pi\mu_0\chi'' H_0^2 \tag{1}$$

where μ_0 − the permeability of free space, H_0 − is the magnetic field intensity in the material, f − the field frequency. This relation can be explained physically that if M lags H we have a positive conversion of magnetic energy supplied with a magnetic field into internal thermal energy.

For a particle in magnetic fluid staying at rest in a low-frequency field, magnetic relaxation process yields the main energy loss. In magnetic relaxation magnetization vector fulfils following differential equation [4]:

$$\frac{dM(t)}{dt} = \frac{1}{\tau}\left[M_\infty(t) - M(t)\right] \tag{2}$$

where M is the magnetization intensity, τ is the relaxation time. When AC excitation field in complex domain has the value $H(t) = H_0 e^{j\omega t}$, then the magnetization in equilibrium state is equal $M_\infty(t) = \chi_0 H_0 e^{j\omega t}$, where χ_0 is susceptibility at rest. Introducing this value into above equation gives

$$M(t) = \frac{\chi_0 H_0}{1 + \mathrm{j}\omega\tau} e^{\mathrm{j}\omega t} \tag{3}$$

Because from definition we have, that

$$M(t) = \hat{\chi} H(t) \tag{4}$$

where $\hat{\chi}$ is complex susceptibility and is given by

$$\hat{\chi} = \chi' - \mathrm{j}\chi'' = \frac{\chi_0}{1 + \mathrm{j}\omega\tau} \tag{5}$$

where the components of susceptibility have the values

$$\chi' = \frac{\chi_0}{1 + (\omega\tau)^2} \tag{6}$$

$$\chi'' = \frac{\omega\tau\,\chi_0}{1 + (\omega\tau)^2} \tag{7}$$

Introducing (7) into (1) gives power losses dissipated in magnetic dissipation process

$$P = 2\pi^2\mu_0\chi_0 H_0^2 f^2 \frac{\tau}{1 + (2\pi f\tau)^2} \tag{8}$$

and its dimension is $\mathrm{W/m^3}$. In magnetic particle, which has a finite size and is placed in constant magnetic field H_{ex}, demagnetizing field H_d is induced by oriented magnetic dipoles. Total filed in particle has lower value

$$H_{tot} = H_{ex} - H_d \tag{9}$$

$$M = \chi_m H_{tot} \tag{10}$$

where χ_m is the magnetic susceptibility of the particle. It can be shown [4] that demagnetizing strength vector is given by

$$\mathbf{M}_d = -\bar{\bar{\mathbf{N}}} \cdot \mathbf{M} \tag{11}$$

where $\bar{\bar{\mathbf{N}}}$ is a demagnetizing factor in tensor form and is given by

$$N_{ij} = -\frac{1}{4\pi}\int_S n_j \frac{x_i - x_i'}{r^3} dS' \tag{12}$$

where n_j are components of unit normal vector to the surface S. When the major axes of the particle coincide with coordinate axes, then for $i \neq j$, $M_{ij} = 0$, and the demagnetizing tensor reduces to

$$\mathbf{H}_d = -\left(\mathbf{a}_1 N_{11} M_1 + \mathbf{a}_2 N_{22} M_2 + \mathbf{a}_3 N_{33} M_3\right) \tag{13}$$

where $\mathbf{a}_i$ are unit versors and where

$$N_{11} + N_{22} + N_{33} = 1 \tag{14}$$

There demagnetizing factors depend only from geometrical shapes of the particles and not from material properties.

When particle has a cylinder shape with radius R_0, and length h, and is placed in uniform magnetic field H_{ex} along the longitudinal axis of the particle then the magnetization is quasi-uniform along this axis. When coordinate axes coincide with cylinder axes, the transversal magnetizations are

$$M_1 = M_2 = 0 \tag{15}$$

and the induced demagnetizing field is uniform along the longitudinal axis and is given by

$$H_d = -N_{33} M_3 \tag{16}$$

The demagnetizing factor along the longitudinal axis N_{33} can be computed from (12) and has a value [4]

$$N_{33} = -\frac{1}{4\pi}\int_S n_3 \frac{x_3 - x_3'}{r^3} dS' = 1 - \frac{h}{\sqrt{h^2 + (2R_0)^2}} \tag{17}$$

Because of the symmetry, the transversal demagnetizing factors are also given by

$$N_{11} = N_{22} = \frac{1 - N_{33}}{2} = \frac{h}{2\sqrt{h^2 + (2R_0)^2}} \tag{18}$$

From (9), (10), and (16), for the assumption of uniform magnetization, we have

$$H_d = \frac{N\chi_m}{1 + N\chi_m} H_{ex} \tag{19}$$

$$H_{tot} = \frac{1}{1 + N\chi_m} H_{ex} \tag{20}$$

where N is the demagnetizing factor for given particle.

When the particle is placed in homogeneous magnetic external AC field $H_{ex}e^{j\omega t}$, then

$$\chi_m = \chi' - \mathrm{j}\chi'' \tag{21}$$

Introduction (21) into (19) and (20) yields [4]:

(22)
$$H_{\mathrm{tot}} = \left|\frac{H_{\mathrm{ex}}}{1+N\chi_{\mathrm{m}}}\right| = \left|\frac{H_{\mathrm{ex}}}{1+N\left(\chi'-\mathrm{j}\chi''\right)}\right| = \frac{H_{\mathrm{ex}}}{\sqrt{\left(1+N\chi'\right)^2+\left(N\chi''\right)^2}}$$

(23)
$$H_{\mathrm{d}} = \left|\frac{N\chi_{\mathrm{m}}H_{\mathrm{ex}}}{1+N\chi_{\mathrm{m}}}\right| = \frac{H_{\mathrm{ex}}N\sqrt{\chi'^2+\chi''^2}}{\sqrt{N^2\left(\chi'^2+\chi''^2\right)+2N\chi'+1}}$$

Relaxation losses

Introducing (22) into (1) gives for the AC magnetization losses with demagnetizing field effects taking into account

(24)
$$P = \pi\mu_0 f\frac{\chi''}{\left(1+N\chi'\right)^2+\left(N\chi''\right)^2}H_{\mathrm{ex}}^2$$

Taking into account (5) and (6) yields

(25)
$$P = 2\pi\mu_0 f^2\frac{\chi_0\tau}{\left(1+N\chi_0\right)^2+\left(\omega\tau\right)^2}H_{\mathrm{ex}}^2$$

The heating power generated by magnetic fluids is primarily from the Brownian and Néel relaxation processes of superparamagnetic particles. In Brownian relaxation process, the magnetic moment vector of particle is attached to the domain and rotates with external field. When placed in an alternating magnetic field, the particle moment rotates together with particle. In Néel relaxation, the magnetic moment rotates within the magnetic domain with the applied magnetic field while crystal structure is fixed. The Brownian relaxation time is given by

(26)
$$\tau_{\mathrm{B}} = \frac{3\eta V_{\mathrm{h}}}{k_{\mathrm{B}}T}$$

and for the Néel process the time relaxation constant has the value

(27)
$$\tau_{\mathrm{N}} = \tau_0\exp\left(\frac{K_{\mathrm{u}}V_{\mathrm{m}}}{k_{\mathrm{B}}T}\right)$$

where η is the viscosity coefficient of the carrier liquid, V_{h} is the hydrodynamic volume of the particle and K_{u} the anisotropy constant of the particles. A value of $\tau_0 = 10^{-9}$ s is mostly used [5]. When in colloid containing superparamagnetic particles, Brownian and Néel processes occur simultaneously, the effective relaxation time τ is given by [2]

(28)
$$\frac{1}{\tau} = \frac{1}{\tau_{\mathrm{B}}}+\frac{1}{\tau_{\mathrm{N}}}$$

For spherical particles we have

(29)
$$V_{\mathrm{m}} = \frac{4}{3}\pi R^3$$

(30)
$$V_{\mathrm{h}} = \frac{4}{3}\pi\left(R+\delta\right)^3$$

where R is the radius of magnetic particle and δ is the coating layer thickness surrounding that particle. Substituting (26) and (27) into (28) and taking into account (29) and (30) we get

(31)
$$\tau = \left[\frac{1}{\tau_0}\exp\left(-\frac{4\pi R^3K_{\mathrm{u}}}{3k_{\mathrm{B}}T}\right)+\frac{k_{\mathrm{B}}T}{4\pi\eta\left(R+\delta\right)^3}\right]^{-1}$$

The typical values and ranges of the material parameters of a magnetite ferrofluid are as follows: field intensity $H_{\mathrm{ex}} < 16\ \mathrm{kA/m}$, with the typical value $8\ \mathrm{kA/m}$, the typical field frequency $f < 1\mathrm{MHz}$ with typical value $100\ \mathrm{kHz}$. The typical temperature is equal $T = 300\ \mathrm{K}$.

Assuming that effective field strength H_{eff} in particle is equal to the external field H_{ex} then the approximate value of the power losses is given by [4]

(32)
$$P_{\mathrm{a}} = \frac{4\pi^2\sigma f^2\tau^2}{1+4\pi^2\tau^2f^2}H_{\mathrm{ex}}\left(\coth\left(\alpha H_{\mathrm{ex}}\right)+\frac{1}{\alpha H_{\mathrm{ex}}}\right)$$

where

(33)
$$\alpha = \frac{4\pi R^3\mu_0M_{\mathrm{d}}}{3k_{\mathrm{B}}T}\ ,\quad \sigma = \frac{\mu_0\psi M_{\mathrm{d}}}{2\tau}$$

The value of $M_{\mathrm{d}} = \psi M_{\mathrm{s}}$, where M_{s} is the saturation magnetization of the particle system ψ is the solid volume fraction of the particles in the whole colloid.

Simulation results

In this section dependence of power losses P_{a} from particle radius is examined. Following values of the particle and suspension are assumed: $\mu_0=4\pi\cdot10^{-7}$ H/m, τ_0=1e-9 s; k_{B} = 1.38e-23 J/K, ψ = 0.01, T = 300 K; M_{d} = 446000 A/m, K_{u} = 32000 J/m^3; η = 1e-3 Pa·s; δ = 2e-9 nm, f =100 kHz, H_{ex} = 8 kA/m, N = 0.004, $Q_{\mathrm{nano}} = P_{\mathrm{a}}\cdot V$, where V is volume of nanoparticles.

Dependence of power P_{a} from particle radius R is given in Fig.1. We can see that highest value of the generated power for given frequency changes with frequency of the excitation. The maximum is shifted in direction of lower frequency values.

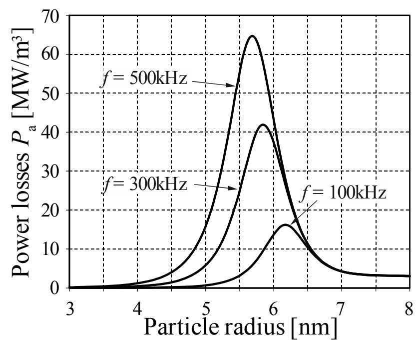

Fig.1. Dependence of the induction heating power on magnetic core size for different particle radius values

Fig.2 shows dependence of P_{a} from viscosity η of the colloid with nanoparticles. For greater viscosity values the power losses diminishes. In this case particles can not rotate so freely as in the case of lower viscosity coefficient. When volume fraction of the particles in suspension in-creases the generated power also get greater value (Fig.3). The above relations were derived with assumption that particles not interact each with other. As one can expect, when strength of the magnetic field increases the generated power also increases (Fig.4). In this way we can control demanding energy supply to human tissues in RF hyperthermia.

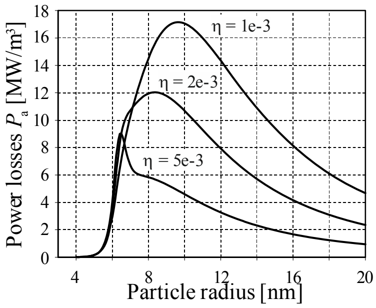

Fig.2. Dependence of the induction heating power from viscosity of the colloid. Dimension of the viscosity η is given in Pa·s

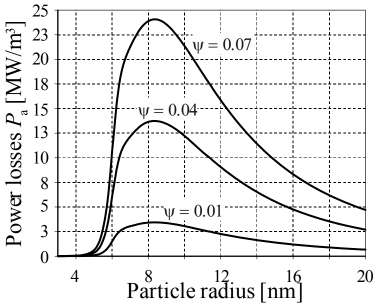

Fig.3. Dependence of the induction heating power from the solid volume fraction of the particles in the whole colloid

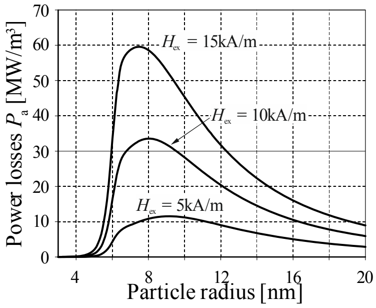

Fig.4. Dependence of the induction heating power from the external magnetic field strength

Equations describing distribution of the electromagnetic field in human body are given by (34) and (35). For detail description of the simulation see [8, 9,10].

$$\nabla \cdot \left(\frac{1}{\mu} \nabla \hat{A}_x \right) + \omega \left(\omega \varepsilon' - \mathrm{j} \left(\sigma + \omega \varepsilon'' \right) \right) \hat{A}_x = -\hat{J}_x \tag{34}$$

$$\nabla \cdot \left(\frac{1}{\mu} \nabla \hat{A}_y \right) + \omega \left(\omega \varepsilon' - \mathrm{j} \left(\sigma + \omega \varepsilon'' \right) \right) \hat{A}_y = -\hat{J}_y \tag{35}$$

Complex permittivity is equal $\hat{\varepsilon}(\omega) = \varepsilon' - \mathrm{j}\varepsilon''$, where $\varepsilon' = \varepsilon_0 \varepsilon_r$ and $\varepsilon'' = \sigma/\omega$. Next magnetic field strength from the following formula has been calculated

$$\hat{\mathbf{H}} = \frac{1}{\mu_0 \mu_r} \left(\frac{\partial}{\partial x} \left(A_{yr} + \mathrm{j} A_{yi} \right) - \frac{\partial}{\partial y} \left(A_{xr} + \mathrm{j} A_{xi} \right) \right) \mathbf{a}_z \tag{36}$$

Table 1. Physical parameters of tissues [6, 9]

Tissue	ε_r	σ [S/m]	k [W/(m·K)]	Q_{met} [W/m³]
human body	29.6	0.053	0.22	300
tumor	160	0.64	0.56	480

Table 2. Physical parameters of blood [9]

Tissue	ρ_b [kg/m³]	C_b [J/(kg·K)]	T_b [K]	ω_b [1/s]
blood	1020	3640	310.15	0.0004

The expression of Pennes bioheat equation in a human body with uniform material properties in steady state magnetic field [11] is given by

$$\nabla \cdot \left(-k \nabla T \right) = \rho_b C_b \omega_b (T_b - T) + Q_{eddy} + Q_{met} + Q_{nano} \tag{37}$$

After solution of the field equations and taken into account power losses given by equation (32) the temperature distribution along tumor perimeter is calculated (Fig.5).

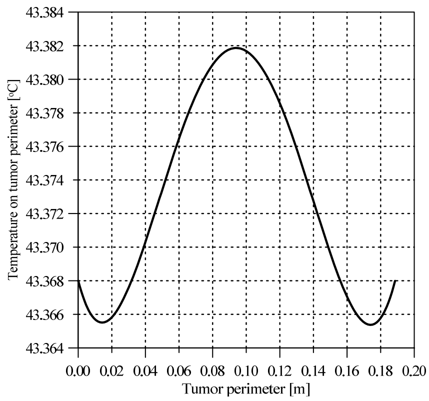

Fig.5. Temperature distribution along the tumor perimeter

REFERENCES

[1] Jordan A., Wust P.,Fahling H., John W., Hinz W., and Felix R., Inductive heating of ferrimagnetic particles and magnetic fluids—Physical evaluation of their potential for hyperthermia, *International Journal of Hyperthermia*, Vol. 9 (1993), No. 1, 51-68.

[2] Hergt R., and Andrä W., Magnetic hyperthermia and thermoablation, in *Magnetism in Medicine: A Handbook*, W. Andrä and H. Nowak, Eds., 2nd ed., Berlin, Wiley-VCH, (2006).

[3] Kurgan E., *Obliczanie sił i momentów w zjawiskach dielektroforezy i magnetoforezy*, Warszawa, BEL Studio, (2013).

[4] Wang X., Tang J., Shi L., Induction Heating of Magnetic Fluids for Hyperthermia Treatment, *IEEE Transactions on magnetics*, Vol. 46 (2010), No. 4, 1043-1051.

[5] Bean C. P. and Livingston J. D., Superparamagnetism, *Journal of Applied Physics*, Vol. 30 (1959), No. 4, 120S–129S.

[6] Gabriel S., Lau R.W., Gabriel C., The dielectric properties of biological tissues: III. Parametric models for the dielectric spectrum of tissues, *Phys. Med. Biol.*, 41 (1996), 2271-2293.

[7] Sawicki B., Miaskowski A., Numerical model of magnetic fluid hyperthermia, *Przeglad Elektrotechniczny*, Vol. 89 (2013), No. 7, 86-88.

[8] Kurgan E., Energy absorption by ferromagnetic nanoparticles in hyperthermia therapy, *Archives of Electrical Engineering*, Vol. 61 (2012), No. 4, 597-608.

[9] Kurgan E., Gas P., Estimation of Temperature Distribution Inside Tissues in External RF Hyperthermia, *Przeglad Elektrotechniczny*, Vol. 86 (2010), No. 01, 100-102.

[10] Gas P., Transient Temperature Distribution inside Human Brain during Interstitial Microwave Hyperthermia, *Przeglad Elektrotechniczny*, Vol. 89 (2013), No. 3a, 274-276.

[11] Pennes H.H., Analysis of Tissue and Arterial Blood Temperatures in the Resting Human Forearm, *Journal of Applied Physiology*, Vol. 1 (1998), No. 85, 5-34.

***Authors**: dr hab. inż. Eugeniusz Kurgan, mgr inż. Piotr Gas, AGH University of Science and Technology, Department of Electrical and Power Engineering, al. Mickiewicza 30, 30-059 Krakow, E-mail: kurgan@agh.edu.pl, piotr.gas@agh.edu.pl*